Clin Orthop Relat Res (2015) 473:3615–3626
DOI 10.1007/s11999-015-4526-0

Clinical Orthopaedics and Related Research®
A Publication of The Association of Bone and Joint Surgeons®

BASIC RESEARCH

Implant Design Variations in Reverse Total Shoulder Arthroplasty Influence the Required Deltoid Force and Resultant Joint Load

Joshua W. Giles PhD, G. Daniel G. Langohr MASc, James A. Johnson PhD, George S. Athwal MD

Received: 17 March 2015 / Accepted: 14 August 2015 / Published online: 27 August 2015

Abstract

Background Reverse total shoulder arthroplasty (RTSA) is widely used; however, the effects of RTSA geometric parameters on joint and muscle loading, which strongly influence implant survivorship and long-term function, are not well understood. By investigating these parameters, it should be possible to objectively optimize RTSA design and implantation technique.

Questions/purposes The purposes of this study were to evaluate the effect of RTSA implant design parameters on (1) the deltoid muscle forces required to produce abduction, and (2) the magnitude of joint load and (3) the loading angle throughout this motion. We also sought to determine how these parameters interacted.

Methods Seven cadaveric shoulders were tested using a muscle load-driven in vitro simulator to achieve repeatable motions. The effects of three implant parameters—humeral lateralization (0, 5, 10 mm), polyethylene thickness (3, 6, 9 mm), and glenosphere lateralization (0, 5, 10 mm)—were assessed for the three outcomes: deltoid muscle force required to produce abduction, magnitude of joint load, and joint loading angle throughout abduction.

Results Increasing humeral lateralization decreased deltoid forces required for active abduction (0 mm: 68% ± 8% [95% CI, 60%–76% body weight (BW)]; 10 mm: 65% ± 8% [95% CI, 58%–72 % BW]; p = 0.022). Increasing glenosphere lateralization increased deltoid force (0 mm: 61% ± 8% [95% CI, 55%–68% BW]; 10 mm: 70% ± 11% [95% CI, 60%–81% BW]; p = 0.007) and joint loads (0 mm: 53% ± 8% [95% CI, 46%–61% BW]; 10 mm: 70% ± 10% [95% CI, 61%–79% BW]; p < 0.001). Increasing polyethylene cup thickness increased deltoid force (3 mm: 65% ± 8% [95% CI, 56%–73% BW]; 9 mm: 68% ± 8% [95% CI, 61%–75% BW]; p = 0.03) and joint load (3 mm: 60% ± 8% [95% CI, 53%–67% BW]; 9 mm: 64% ± 10% [95% CI, 56%–72% BW]; p = 0.034).

Conclusions Humeral lateralization was the only parameter that improved joint and muscle loading, whereas glenosphere lateralization resulted in increased loads. Humeral lateralization may be a useful implant parameter in countering some of the negative effects of glenosphere

One or more of the authors (JWG, GDGL) has received research funding from the Natural Science and Engineering Research Council of Canada (Ottawa, Ontario, Canada). The institution of one or more of the authors (JAJ) has received, during the study period, funding from the Natural Science and Engineering Research Council of Canada.
All ICMJE Conflict of Interest Forms for authors and *Clinical Orthopaedics and Related Research*® editors and board members are on file with the publication and can be viewed on request.
Clinical Orthopaedics and Related Research® neither advocates nor endorses the use of any treatment, drug, or device. Readers are encouraged to always seek additional information, including FDA-approval status, of any drug or device prior to clinical use.
Each author certifies that his or her institution approved the human protocol for this investigation, that all investigations were conducted in conformity with ethical principles of research, and that informed consent for participation in the study was obtained.
This work was performed at the Bioengineering Laboratory of the Roth McFarlene Hand and Upper Limb Centre, London, Ontario, Canada.

J. W. Giles (✉), G. D. G. Langohr, J. A. Johnson, G. S. Athwal
Roth McFarlane Hand and Upper Limb Centre, 268 Grosvenor Street, London, ON N6A 4V2, Canada
e-mail: giles.joshgiles@gmail.com; joshua.giles@imperial.ac.uk

J. W. Giles, G. D. G. Langohr, J. A. Johnson, G. S. Athwal
Western University, London, ON, Canada

J. W. Giles
Mechatronics in Medicine Laboratory, Department of Mechanical Engineering, Imperial College London, London, UK

lateralization, but this should not be considered the sole solution for the negative effects of glenosphere lateralization. Overstuffing the articulation with progressively thicker humeral polyethylene inserts produced some adverse effects on deltoid muscle and joint loading.

Clinical Relevance This systematic evaluation has determined that glenosphere lateralization produces marked negative effects on loading outcomes; however, the importance of avoiding scapular notching may outweigh these effects. Humeral lateralization's ability to decrease the effects of glenosphere lateralization was promising but further investigations are required to determine the effects of combined lateralization on functional outcomes including range of motion.

Introduction

Despite the widespread use of reverse total shoulder arthroplasty (RTSA) [1, 11, 27], the fundamental effects of implant configuration on certain biomechanical outcomes have not been completely elucidated. The deltoid muscle force required to produce active motion and the resulting joint load magnitude and angle throughout this motion are important factors when considering the potential effect of implant configuration on long-term RTSA performance. Specifically, after RTSA, arm elevation primarily is dependent on the deltoid, but large increases in this muscle's force may be associated with acromial fracture and chronic muscle fatigue [8, 15, 30, 32]. In addition, increased joint loading has been linked with greater implant wear and fixation failure [4]. Initial research in the biomechanical performance of RTSA focused on individual commercially available implant configurations [2, 3, 19, 22, 28], although some studies have addressed individual design parameters at numerous values (such as humeral version at 10°, 20°, 30°) [16–18, 24]; however, there are little data regarding how these parameters interact with one another and influence joint and muscle-loading outcomes.

The configuration of an RTSA is defined by many geometric parameters; however, three parameters were chosen for this study that were thought to have the most direct influence on muscle moment arms, and thus loading outcomes: glenosphere lateralization, humeral lateralization, and polyethylene cup thickness. Glenosphere lateralization is commonly used to eliminate impingement between the humeral component and glenoid bone but it also causes a decrease in the deltoid's moment arm and thus its ability to effectively elevate the arm [17]. Humeral lateralization—which may improve the deltoid moment arm and joint compressive load—has become adjustable in numerous implant systems, with each offering a different level of lateralization. Finally, polyethylene cup thickness is frequently adjusted to optimize passive joint tension and stability, but its effects on other outcomes are unknown [18], especially if the joint is overtensioned (overstuffed).

The purpose of this investigation was to provide a more systematic understanding of the fundamental effects of glenosphere and humeral component design parameters on the deltoid force required to achieve active abduction and on the joint load magnitude and angle throughout this motion. We hypothesized that (1) the deltoid force required to produce active motion would be increased by glenosphere lateralization, be decreased by humeral lateralization, and be unaffected by changes in humeral polyethylene cup thickness. (2) The joint load magnitude resulting from active motion would be affected by each implant parameter in the same way as in the first hypothesis. (3) The joint load angle would be unaffected by glenosphere lateralization, become more compressive with increasing humeral lateralization, and be unaffected by changes in humeral polyethylene cup thickness.

Materials and Methods

Custom Adjustable RTSA System

To test our hypotheses independent of the limited implant configurations achievable using commercial implant systems and to produce generalizable findings, we designed custom humeral (Fig. 1) and glenoid (Fig. 2) components with multiple levels of adjustability for each geometric parameter of interest. The glenoid and humeral components were also designed with interchangeable glenosphere and humeral cup sizes and allowed adjustment of glenosphere inferiorization, humeral head-neck angle, and humeral anteversion-retroversion. The glenoid component also incorporates a six-axis load sensor to measure transarticular forces and moments.

Humeral Component

A commercially available polyethylene insert (+3 mm; Delta XTEND^{TM}, DePuy Synthes, Warsaw, IN, USA) was used (Fig. 1A). The humeral implant was composed of three custom-adjustable or interchangeable components. Three millimeter-thick disc-shaped spacers (Fig. 1B-2) could be placed beneath the humeral cup to adjust its effective thickness (0, 1, or 2 spacers corresponding to thicknesses of 3, 6, or 9 mm). These spacers were in turn attached to a head-neck component (Fig. 1C) that could be interchanged to adjust the implants head-neck angle.

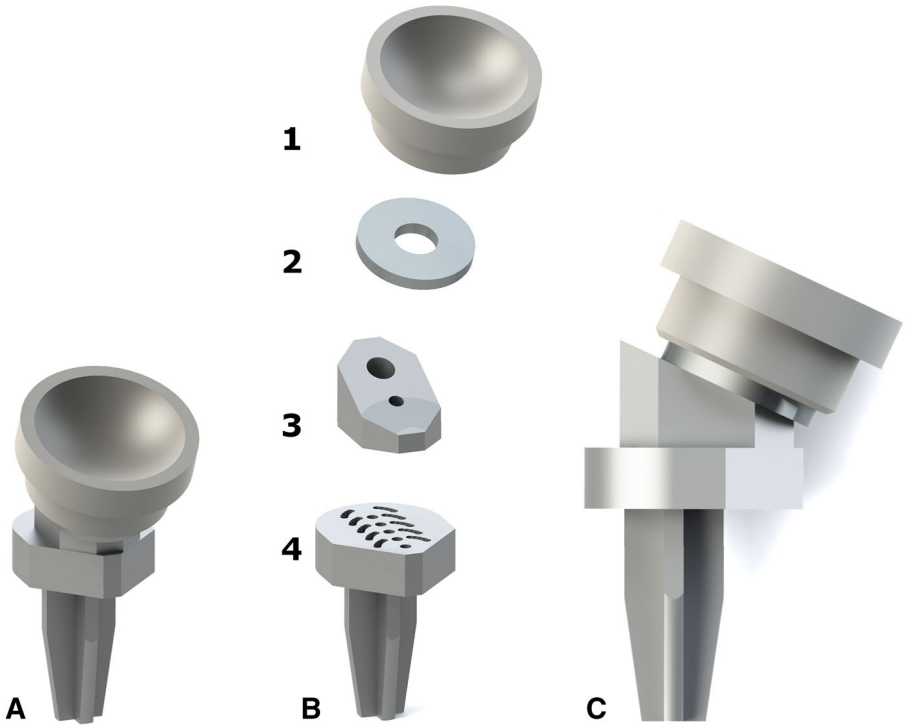

Fig. 1A–C (**A**) An isometric computer rendering of the custom modular humeral implant is shown. (**B**) The middle images show an isometric exploded view of the humeral implant with the modular components separated: a +3-mm polyethylene cup (Delta XTEND^{TM}, DePuy) (1), a humeral spacer which produces changes in humeral cup thickness in increments of 3 mm (2), a 155° head-neck angle component (3), and a humeral stem and baseplate component which facilitates cup adjustability through the use of retroversion dowel holes spaced at 5° (0°–20°), and threaded holes for lateralization of the humeral shaft spaced at 5 mm (−5 to +15 mm) (4). (**C**) A side view of the component shows its 155° head-neck angle.

Finally, the head-neck component is bolted into one of multiple configurations provided by the humeral baseplate-stem component (Fig. 1B-4). In this way, the head-neck component is used to adjust humeral shaft lateralization by bolting it to the humeral stem at any one of a series of threaded holes spaced in 5-mm increments running mediolaterally (Fig. 1B-4).

Glenoid Component

A custom-designed 38-mm glenosphere was machined and finished to a moderate polish (Fig. 2A). Lateralization spacer(s) (each 5 mm thick) (Fig. 2B-2) can be interposed between the glenosphere and a six degrees-of-freedom load cell (Nano25; ATI Industrial Automation, Apex, NC, USA) (Fig. 2C-3)—which is used to measure transarticular forces and moments—that in turn connects to a fixation baseplate (Fig. 2C-4). The glenosphere–load-cell–baseplate construct, with no lateralization spacers, corresponds to a 0-mm glenosphere lateralization configuration. The baseplate was fixed in the glenoid vault using three 4.5-mm screws.

Specimen Preparation

Seven fresh-frozen cadaveric shoulders (mean ± SD, 71 ± 10 years; range, 56–84 years) were tested. The humerus was transected midshaft, and a full-thickness supraspinatus and upper infraspinatus tear was created. To allow joint access during implantation and configuration changes, the subscapularis muscle was elevated and reflected laterally.

The custom RTSA system was implanted using a modified technique from the DePuy product manual [9]. The neutrally configured humeral component was cemented in the standard RTSA position of 0° retroversion relative to the epicondyles. By using a guide, the glenosphere baseplate's inferior edge was made to coincide with the inferior glenoid and was secured after appropriate reaming to accommodate the baseplate–load-cell construct.

To permit dynamic muscle force application, the three heads of the deltoid were sutured separately at the deltoid insertion using a transosseous technique, whereas a running locking stitch was used to suture the musculotendinous junctions of the lower infraspinatus and teres minor together as one unit, and separately for the subscapularis muscle. The remainder of specimen preparation was

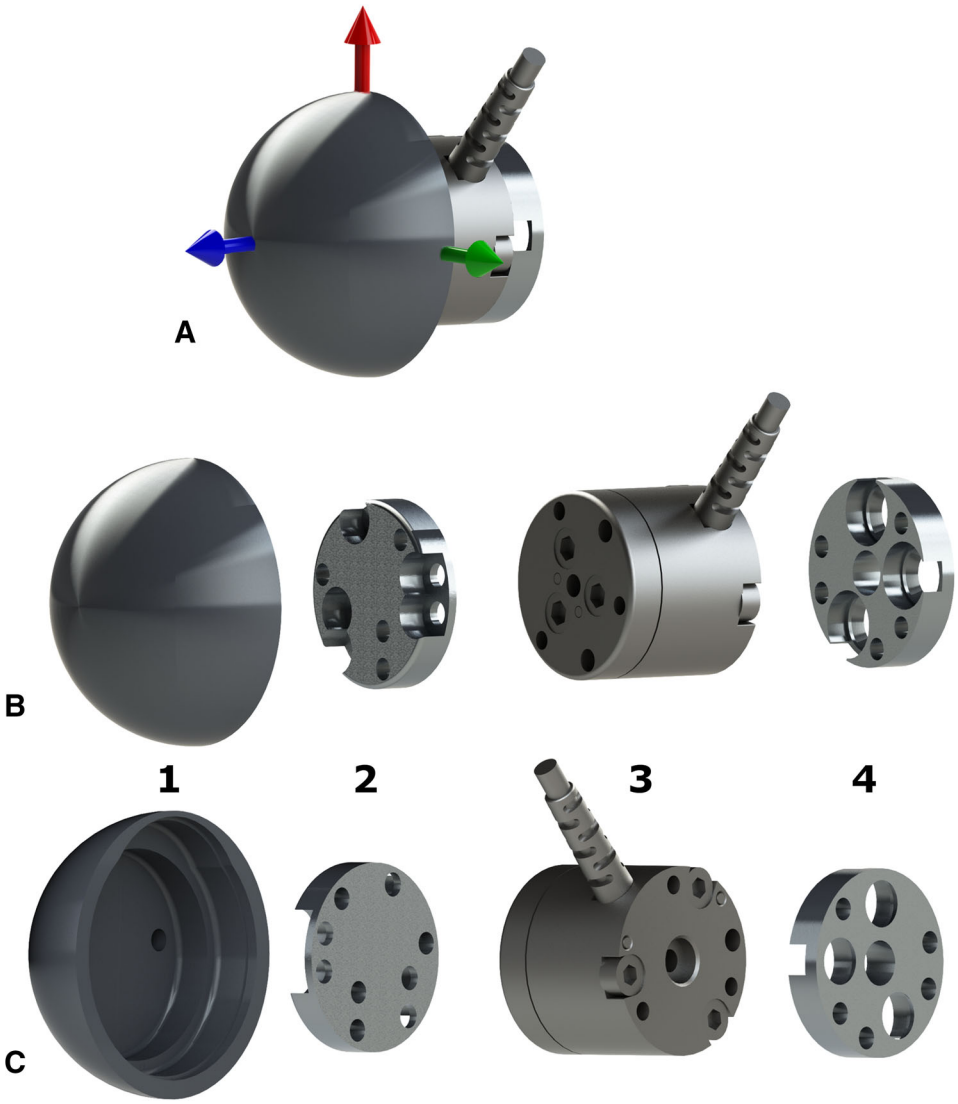

Fig. 2A–C A computer rendering of the custom modular glenoid implant shows (**A**) an isometric view of the assembled glenosphere components with coordinate frame indicating the load measurement directions; (**B**) an isometric exploded view of the four glenoid components separated: a custom 38-mm diameter hemispheric glenosphere component with hollowed-out back (1), a 5-mm (also 0 and 10 mm) glenosphere lateralization spacer which nests in the hollow of 1 (2), a six-axis load sensor designed to nest in the hollow of 1 and in the reamed glenoid fossa (3), and a glenosphere baseplate for fixation of the glenoid implant to the scapula (4); and (**C**) the reverse angle of the isometric exploded view.

completed as described previously [11], which included fixation of optical trackers (OptoTrak Certus™, NDI, Waterloo, Canada) to the scapula and insertion of an optically tracked intramedullary humeral rod. Humeral and scapular anatomic digitizations were taken to create physiologically relevant coordinate systems [34] for use in the real-time control of joint motion and in post hoc data analysis. The load cell's coordinate system also was digitized, whereas the glenosphere and humeral cup centers of rotation were determined from kinematic recordings [33] to transform recorded loads into a glenoid coordinate system located at the RTSA rotation center for each configuration (Fig. 2A).

Simulator Testing Apparatus

The scapula of the prepared specimen was cemented onto a validated in vitro shoulder simulator (Fig. 3) [12] that applied forces to each of the remaining cuff muscles and the three deltoid heads along physiologically accurate lines of action through the use of five independently computer-controlled pneumatic actuators. By using real-time kinematic data and a multi- Proportional-Integral-Derivative (PID) control system [13], the applied muscle forces are continually modulated, thus allowing predefined muscle-driven active motion profiles to be accurately and repeatably produced. Reported muscle loading ratios [21] were

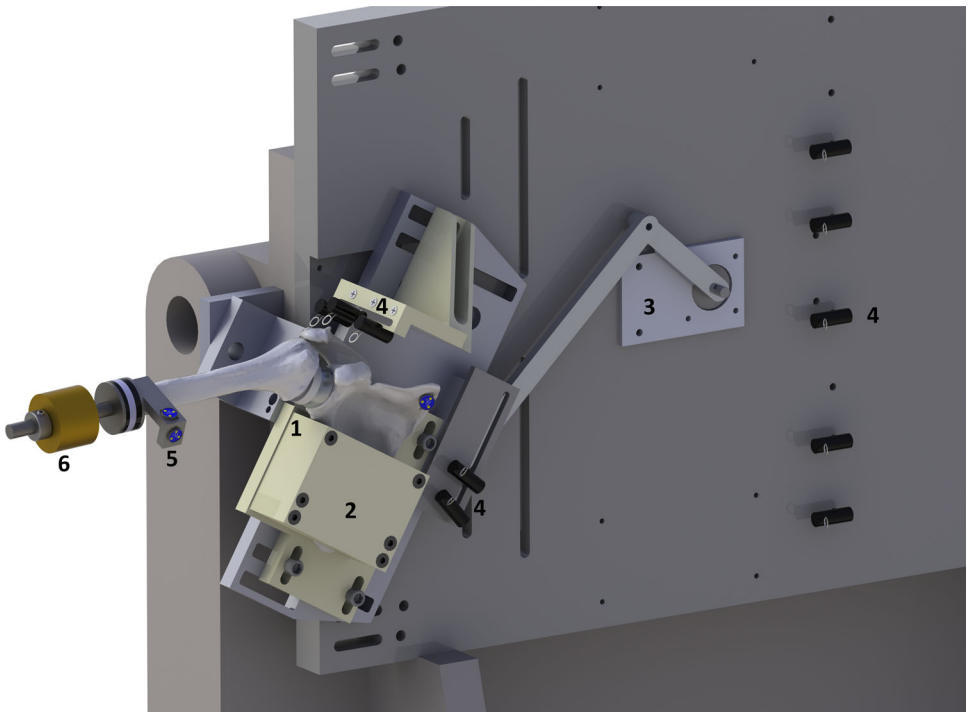

Fig. 3 A computer rendering of the in vitro muscle loading-driven active motion simulator with a right shoulder mounted shows: a scapula and humerus implanted with the custom adjustable, instrumented RTSA prosthesis (1); rotating scapula pot (2); motor and linkage mechanism to drive scapula pot rotation (3), low-friction deltoid and rotator cuff cable guide system which routes sutures from the muscle attachment to low friction pneumatic actuators (out of frame to the right) (4), optical trackers used to provide real-time kinematic feedback to the control system (5), and weight used to replace the mass of the resected distal arm (6). Soft tissues are omitted for clarity.

used to guide the forces the simulator applied, thus ensuring they accurately replicated in vivo values; however, the control system modulated the precise values of these ratios to enable each specimen to achieve the predefined motion despite interspecimen variability. In addition to generating glenohumeral motion, the simulator produced physiologically accurate scapular elevation rotations in rhythm with the glenohumeral orientation using a previously validated motor and linkage-driven rotating scapula pot. Replication of the shoulder's in vivo glenohumeral-to-scapulothoracic rhythm is critical in producing accurate glenohumeral articular kinematics [13].

Experimental Protocol

Twenty-seven implant configurations—all permutations of the three parameters each at three levels—were evaluated in random order: (1) glenosphere lateralization 0, 5, 10 mm; (2) polyethylene thickness 3, 6, 9 mm; and (3) humeral lateralization 0, 5, 10 mm. Each parameter's smallest value corresponded to the clinically neutral configuration whereby the glenosphere's base was flush with the glenoid, the humeral cup's rim was in line with the greater tuberosity's upper aspect, and the humeral cup's deepest point was 12.5 mm medial to the humeral shaft as is the case in a standard Grammont-style RTSA (ie, 155° head-neck angle, with inlay of the component in the metaphysis and not markedly medializing the cup relative to the humeral shaft) [7]. All other parameters were held constant: glenosphere and humeral cup size = 38 mm, glenosphere inferiorization = 0 mm, humeral head-neck angle = 155°, humerus retroversion = 0°.

For each configuration, active scapular plane abduction was simulated from 0° to 90° humerothoracic rotation at a rate of 1° per second. During this motion, scapular rotation was dictated by the 2:1 glenohumeral-to-scapulothoracic rhythm described by Inman et al. [20]. This traditionally accepted ratio was chosen because there continues to be disagreement regarding if and/or how RTSA alters scapular rotation. One study showed that patients who had RTSA exhibited greater scapular rotation [23], whereas another showed little change or even a decrease in rotation [25]. Muscle and other soft tissues were hydrated regularly using normal saline throughout the testing protocol.

Table 1. Summary of implant parameters with significant main effects

Geometric parameter levels	Deltoid load (% BW)			Joint load (% BW)			Joint load angle (°)
	Humeral lateralization	Polyethylene cup thickness	Glenosphere lateralization	Humeral lateralization	Polyethylene cup thickness	Glenosphere lateralization	Humeral lateralization
	Main effects						
	p = 0.004 Pairwise comparisons	p = 0.012	p = 0.002	p = 0.275	p = 0.007	p < 0.001	p < 0.001
1st configuration level	68 ± 8*	65 ± 9*	61 ± 7*,†	62 ± 8	60 ± 9*	53 ± 7*,†	37 ± 12*,†
2nd configuration level	66 ± 8	67 ± 8†	67 ± 7*	62 ± 8	61 ± 8†	62 ± 7*,‡	35 ± 11*,‡
3rd configuration level	65 ± 8*	68 ± 8*,†	70 ± 11†	61 ± 7	64 ± 8*,†	70 ± 11†,‡	31 ± 11†,‡

1st, 2nd, and 3rd configuration levels correspond to 0, 5, and 10 mm configuration levels for subsequent columns labeled Humeral lateralization and Glenosphere lateralization, and to 3, 6, and 9 mm for columns labeled Polyethylene cup thickness; *,†, ‡ signify significant comparisons between the indicated implant parameter levels (eg, 0 mm and 5 mm) with p < 0.05.

Outcome Variables and Statistics

Three outcomes were assessed across active abduction. First, deltoid muscle force was evaluated by summing the magnitude of the force applied by each of the three heads. Second, joint load magnitude was calculated after transforming the loads (Cartesian forces and torques) measured by the glenosphere load cell into a glenoid coordinate system located at the glenosphere center. Deltoid force and joint load were converted to percentage body weight (% BW) by dividing by the donor's total weight. Third, joint loading direction in the scapular plane was calculated using the transformed superior (y) and lateral (z) joint loads, where 0° is a purely compressive force and positive angles are upwardly directed forces. Each outcome was assessed at 5°-increments between 22.5° and 82.5° of humerothoracic abduction, a range that all configurations achieved.

A four-way (glenosphere lateralization, polyethylene thickness, humeral lateralization, abduction angle) repeated-measures ANOVA was performed for each of the outcomes (SPSS Version 16.0; SPSS Inc, Chicago, IL, USA). Pairwise comparisons, which were adjusted using the Bonferroni correction, and analyses of interactions were performed for cases showing a significant effect ($p < 0.05$). A priori sample-size calculations for each outcome showed that seven specimens were sufficient to achieve 80% or greater power using our repeated measures study design for clinically meaningful differences of 5% BW and 5° for the respective outcomes.

Results

Deltoid Muscle Force

Humeral lateralization resulted in decreased deltoid force (p = 0.004), whereas glenosphere lateralization (p = 0.002), thicker polyethylene (p = 0.012), and a higher abduction angle ($p < 0.001$) resulted in increased deltoid force (Table 1). Deltoid muscle force varied across active abduction for the differing levels of humeral and glenosphere lateralization (Fig. 4). Specifically, decreases in deltoid force were observed when humeral lateralization was increased from 0 mm to 10 mm (0 mm: 68% ± 8% [95% CI, 60%–76% BW]; 10 mm: 65% ± 8% [95% CI, 58%–72% BW]; p = 0.022). As glenosphere lateralization increased from 0 mm (61% ± 8% [95% CI, 55%–68% BW]), increases in deltoid force were required to abduct the arm (5 mm: 67% ± 8% [95% CI, 61%–73% BW], p = 0.01; 10 mm: 70% ± 11% [95% CI, 60%–81% BW], p = 0.007). Similarly, as polyethylene thickness increased from 3 mm (65% ± 8% [95% CI, 56%–73% BW]) increases in deltoid force were required to abduct the arm (6 mm: 67%

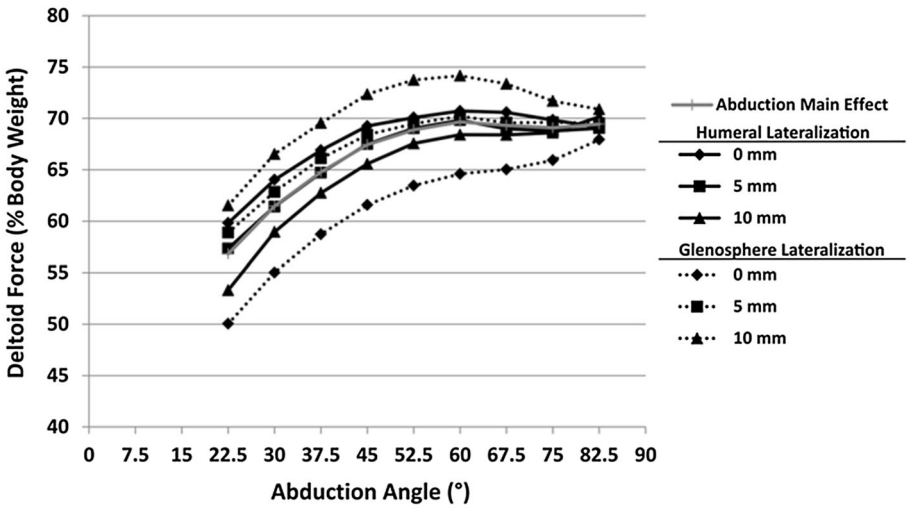

Fig. 4 Implant parameters whose effects on the deltoid force varied across abduction are shown. The means (SDs omitted for clarity) of deltoid force averaged across all levels of the geometric parameters (Abduction Main Effect) and for differing levels of humeral and glenosphere lateralization (0, 5, 10 mm) are shown. SDs range from 4% to 16% body weight.

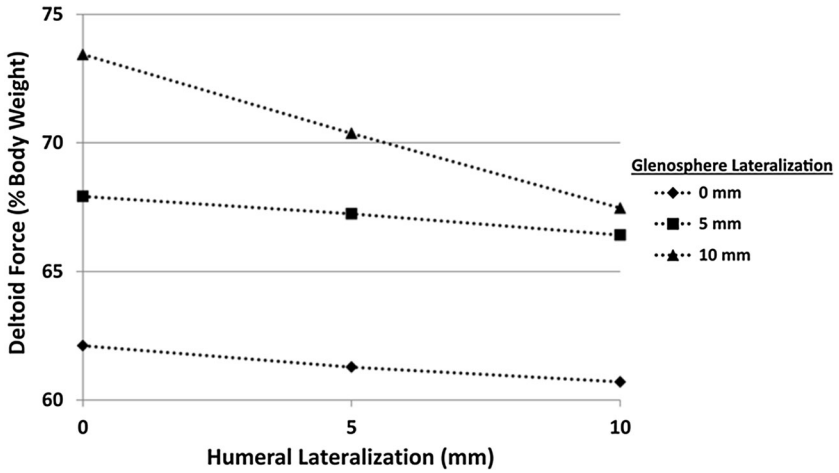

Fig. 5 The deltoid force interaction between humeral and glenosphere lateralizations is shown. The data represent means (SDs omitted for clarity) of deltoid force averaged across abduction and humeral cup thickness for changes in humeral and glenosphere lateralization. SDs range from 6% to 12% body weight.

± 8% [95% CI, 59%–74% BW], p = 0.006; 9 mm: 68% ± 8% [95% CI, 61%–75% BW], p = 0.03).

Humeral and glenosphere lateralization were found to interact (p = 0.03) such that deltoid muscle force decreased with increasing humeral lateralization and humeral lateralization's reductive effect was increased as glenosphere lateralization increased (Fig. 5). Humeral lateralization's increasing reductive effect with increasing levels of glenosphere lateralization caused the comparisons at 5 and 10 mm of humeral lateralization to not be different between the 5- and 10-mm glenosphere lateralizations (differences less than 3% ± 4%–7% BW; p ≥ 0.878). Conversely, all other increases in glenosphere lateralization produced increases in deltoid force (differences greater than 6% ± ≤ 2%–7% BW; p ≤ 0.031) (Fig. 5). However, these force reductions could not decrease the deltoid force to the level measured with 0 mm glenosphere lateralization (10 mm of glenosphere and humeral lateralization: 67% ± 11% [95% CI, 58%–77% BW]; 0 mm glenosphere and humeral lateralization: 62% ± 7% [95% CI, 55%–69% BW]).

Joint Load

Thicker polyethylene cups (p = 0.007), glenosphere lateralization (p < 0.001), and moving from adduction into abduction (p = 0.033) all resulted in increased joint loads,

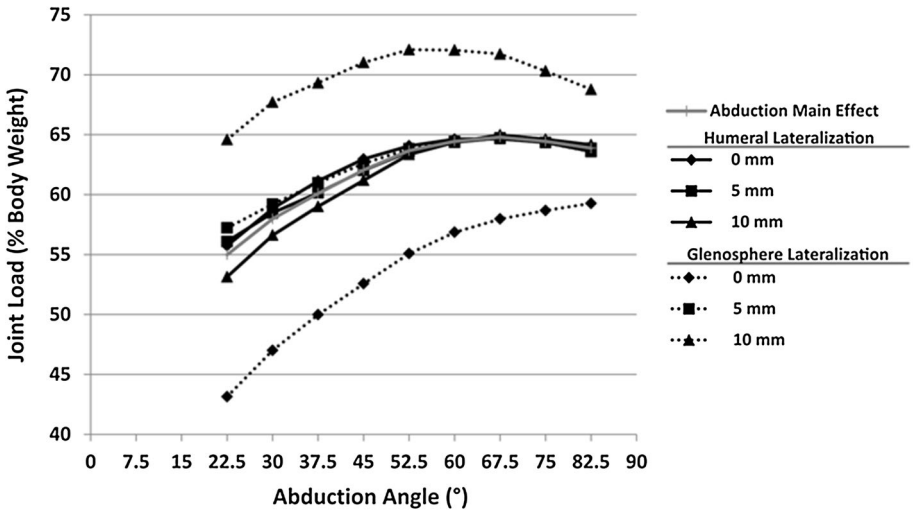

Fig. 6 The implant parameters whose effects on joint load varied across abduction are shown. The data represent the mean (SDs omitted for clarity) joint load averaged across all levels of the geometric parameters (Abduction Main Effect) and for differing levels of humeral and glenosphere lateralization (0, 5, 10 mm). SDs range from 7% to 12% body weight.

but humeral lateralization did not ($p = 0.275$) (Table 1). Specifically, joint load increased for each increase in glenosphere lateralization (0 mm: 53% ± 8% [95% CI, 46%–61% BW]; 5 mm: 62% ± 7% [95% CI, 55%–69% BW]; 10 mm: 70% ± 10% [95% CI, 61%–79% BW]; 0 mm vs 5 mm: $p < 0.001$, 0 mm vs 10 mm: $p < 0.001$, 5 mm vs 10 mm: $p = 0.007$). With each additional 5 mm of glenosphere lateralization, joint load increased by a minimum of 7% BW. Additionally, joint load increased with progressively thicker polyethylene cups (3 mm: 60% ± 8% [95% CI, 53%–67% BW]; 6 mm: 61% ± 7% [95% CI, 54%–69% BW]; 9 mm: 64% ± 10% [95% CI, 56%–72% BW]; 3 mm vs 9 mm: $p = 0.034$, 6 mm vs 9 mm: $p = 0.026$). Finally, although joint loads increased as the shoulder abducted (Fig. 6), glenosphere lateralization interacted ($p = 0.003$) with abduction such that the effect of increasing this parameter was moderated as abduction progressed.

Joint Load Angle

Increasing humeral lateralization ($p < 0.001$) and abducting the arm ($p < 0.001$) decreased the joint loading angle (ie, produced a more centrally directed compressive load) (Table 1), whereas glenosphere lateralization interacted with abduction ($p = 0.012$) such that increased lateralization decreased the joint load angle only at low abduction levels (Fig. 7). All pairwise comparisons among the three humeral lateralization levels were different (0 mm: 39° ± 11° [95% CI, 28°–49°; 5 mm: 36° ± 11° [95% CI, 26°–46°; 10 mm: 33° ± 11° [95% CI, 23°–43°]; 0 mm vs 5 mm: $p = 0.006$, 0 mm vs 10 mm: $p < 0.001$, 5 mm vs 10 mm: $p < 0.001$).

Discussion

RTSA is successful because it medializes the glenohumeral center of rotation, thus increasing the mechanical advantage of the remaining muscles, primarily the deltoid [14]. Subsequent to the design of the first commercially viable RTSA prosthesis, numerous implant parameters have been altered in the hopes of improving efficacy and minimizing clinical problems such as scapular notching. However, the effects of changes in these parameters on deltoid force and joint load have not been investigated systematically beyond the configurations available in commercial implants. Three major conclusions, which are largely in agreement with our hypotheses, can be drawn by considering the outcomes of the current systematic investigation of RTSA geometric parameters. First, glenosphere lateralization is often used to eliminate scapular notching; however, caution is required because, as was hypothesized, increasing glenosphere lateralization produced correspondingly negative effects on joint and muscle loading, which influences the long-term success of RTSAs. Second, humeral lateralization may be a promising parameter to optimize RTSA biomechanics, because, as hypothesized, it had positive or neutral effects on all outcomes tested. Additionally, humeral lateralization may be a useful tool in countering some of the negative effects of glenosphere lateralization but this must be investigated further. Third, it was hypothesized that polyethylene thickness would have no effect on outcomes, but

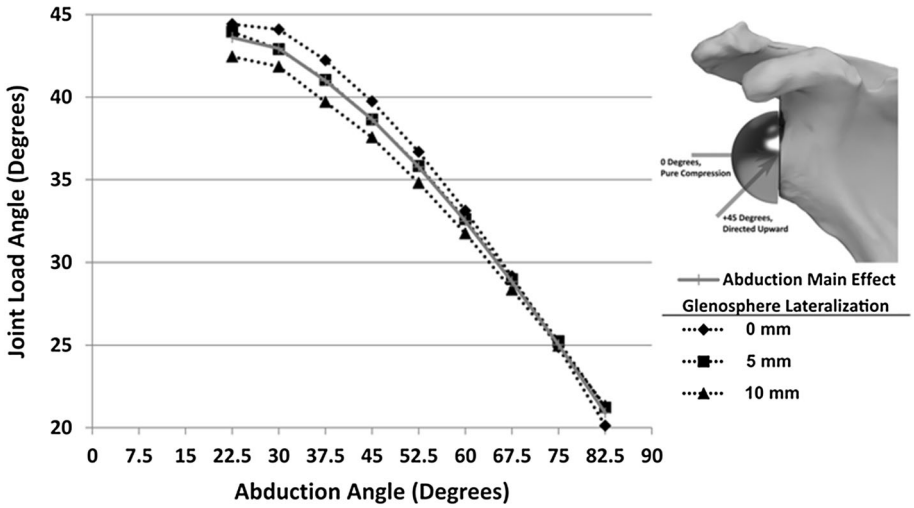

Fig. 7 The changes in joint load angle across abduction are shown. The data represent the means (SDs omitted for clarity) of joint load angle averaged across all levels of the geometric parameters (Abduction Main Effect) and for differing levels of glenosphere lateralization (0, 5, 10 mm), which produced a significant interaction with abduction whereby lateralization decreased load angle early during abduction but had no effect at the end of motion. SDs range from 10° to 13°.

it was found to produce articular overstuffing that had unfavorable effects on deltoid muscle and joint loading, and which must be considered when adjusting joint stability intraoperatively.

The limitations of this study include that it is an in vitro cadaveric investigation which means that all data represent a time-zero case precluding any effect of healing and tissue relaxation with time. As a result, it is possible that some portion of the observed changes in joint loading may be a result of passive overtensioning which may dissipate as tissues relax with time. Additionally, there are many parameters (eg, glenosphere inferiorization, humeral version) that define the configuration of an RTSA, of which only three were varied. Furthermore, interpretation of the presented results must be made with thresholds of clinical importance in mind, not simply statistical significance; however, for the measured outcomes, no such limits have been defined in the literature and thus those used here (5% BW and 5°) should be considered a best estimate. Despite these limitations, the results of this systematic investigation provide a foundation for understanding the effects and interactions of RTSA implant parameters.

In comparing our deltoid force results with those of Ackland et al. [3] and Kontaxis and Johnson [22], our forces are larger (67% BW versus 37% BW and 45% BW, respectively). However, these studies modeled RTSA with complete rotator cuff deficiency, whereas our model involved actively loading the remaining cuff. With this experimental difference in mind, our greater deltoid forces can be explained in light of the work of Ackland et al. [2], who, for one RTSA implant configuration, showed that the rotator cuff's native abduction moment arm is transformed to an adduction effect after RTSA. Our results also show that this inverted effect is especially pronounced early during abduction where the remaining rotator cuff portions—which, in the intact joint, are important in abduction initiation—in fact resist motion and thus cause even greater required deltoid forces early in motion. Additionally, increases in glenosphere lateralization and polyethylene thickness increased the required deltoid force, whereas increases in humeral lateralization decreased it. As hypothesized, glenosphere lateralization increased deltoid force (eg, 10 mm of lateralization increases the force by 9% BW) because it reduced the intended effect of RTSA by decreasing the deltoid's mechanical advantage. This effect is particularly concerning because despite this testing protocol only testing basic arm elevation, glenosphere lateralization elicited a large increase in deltoid loading (ie, approximately 16 pounds [71 N] for an average North American male weighing 178 pounds [31]) which would be further exacerbated by more demanding tasks such as lifting. The effect of lateralizing the glenosphere by 10 mm also may be concerning as this level of offset has been popularized (eg, the bony increased-offset reversed shoulder arthroplasty technique of Boileau et al. [6]) and is endorsed in some product technical manuals [10, 29] as a means to reduce scapular notching. Conversely, humeral lateralization is the only parameter in this model that decreased deltoid force and thus should be an important consideration when designing implants to address the clinical problems of deltoid fatigue and acromial fracture, which are both associated with increased deltoid force [8, 15, 30]. Humeral polyethylene cup thickness was found to have a small effect on deltoid load that approached our

threshold for clinical significance (5% BW). These increases are believed to be caused by a decreased deltoid moment arm and increased cuff adduction moment arm resulting from the greater tuberosity being shifted distally. Therefore, the findings of this study suggest that during surgery, polyethylene thickness should be chosen based on the minimum thickness required to achieve joint stability, as further increases only serve to unnecessarily increase deltoid muscle forces. However, further studies are required to determine the optimum balance between maximizing joint stability and minimizing deltoid forces.

Deltoid force results also showed an interaction between humeral and glenosphere lateralization that, although intuitive, has not been reported previously, to our knowledge. This interaction indicates that increasing humeral lateralization can be used to counter the greater deltoid force requirements associated with increased glenosphere lateralization and that this countering effect is strongest when the glenosphere is lateralized by 10 mm. However, this effect cannot fully reverse the deleterious effect of glenosphere lateralization; a still clinically significant increase of approximately 5% BW remains after humeral lateralization. Thus, humeral lateralization should not be considered a valid means to completely compensate for excessive glenosphere lateralization but may offer a way to limit the incidence of deltoid fatigue and acromial fracture when glenosphere lateralization is used to avoid scapular notching.

As with deltoid force, our simulation of partial cuff deficiency resulted in joint loading values that were greater than those reported by Ackland et al. [3] (65% BW versus 29% BW at 90° abduction) and somewhat higher than the computational results of Kontaxis and Johnson [22] (50% BW at 100° abduction). Our results, however, were similar to those in a computational study by Terrier et al. [28] (60% BW), who also simulated partial cuff deficiency. Despite humeral lateralization's effect of reducing required deltoid force, it did not markedly reduce joint load magnitude. However, joint load did increase after increases in humeral polyethylene thickness and glenosphere lateralization. Increasing polyethylene thickness only increased joint load by approximately 3% BW from the 3-mm to 9-mm configurations, which may not represent a clinically meaningful change. Glenosphere lateralization, however, increased joint load by approximately 16% BW from its 0- to 10-mm configuration with the greatest effect measured at the initiation of active abduction and a moderately decreasing effect as motion progressed. As noted above, this effect would be further exacerbated by more challenging daily tasks which involve resistive loads. These large increases in joint loading, which correspond to approximately 25% of the in vivo joint load measured by Bergmann et al. [5] after primary TSA, may lead to increased polyethylene wear, as was observed by Nam et al. [26], and will increase the loads experienced at the glenosphere baseplate, which has the potential to negatively affect fixation [35]. This, therefore, adds additional evidence in support of the potentially damaging side effects caused by decreasing the effectiveness of the shoulder's musculature through the use of glenosphere lateralization. However, although this effect does appear to be clinically meaningful and may have long-term implications on implant survival, the need to avoid scapular notching may necessarily outweigh this concern. Previous rigid body computational investigations have identified alternative variables (eg, glenosphere inferiorization and tilting) that can effectively reduce scapular notching [22]; therefore, future studies should evaluate the effects of these parameters on muscle and joint loading to determine if they can produce a more optimal compromise between these clinical and biomechanical considerations.

The joint loading angle in the scapular plane was found to be affected only by changes in humeral lateralization. Increases in humeral lateralization decreased average load angle from approximately 37° to approximately 31° over a 10 mm change. These findings further support the use of humeral lateralization as a means to limit the negative effects of joint loading by producing a load vector that is more compressive and thus less challenging to baseplate fixation.

This systematic evaluation of the effects of RTSA geometric parameters on shoulder loading outcomes has provided some important insights which can influence the clinical use of RTSA and of future implant system designs. Of greatest importance is the markedly negative effects that glenosphere lateralization has on loading outcomes which clinicians must be aware of when using this variable to prevent scapular notching. Additional biomechanical investigations should be conducted to identify more optimal methods to avoid this clinical complication without sacrificing RTSA biomechanics. Furthermore, clinical investigations are required to elucidate glenosphere lateralization's long-term effects on function and survivorship. We also identified a previously undescribed beneficial interaction between humeral and glenosphere lateralization which makes the former parameter a good method to counter the latter's negative effects. Further investigations should be conducted to determine what, if any, effect the combination of these parameters has on shoulder function including range of motion. Finally, although this investigation was conducted using a custom implant system, all of the variables studied are readily modifiable in most modern RTSA systems or through surgical technique and thus can be directly translated regardless of the specific commercial system used clinically.

Acknowledgments We thank DePuy (Warsaw, IN, USA) for providing the humeral polyethylene inserts used in this study.

References

1. Acevedo DC, Vanbeek C, Lazarus MD, Williams GR, Abboud JA. Reverse shoulder arthroplasty for proximal humeral fractures: update on indications, technique, and results. *J Shoulder Elbow Surg.* 2014;23:279–289.
2. Ackland DC, Roshan-Zamir S, Richardson M, Pandy MG. Moment arms of the shoulder musculature after reverse total shoulder arthroplasty. *J Bone Joint Surg Am.* 2010;92:1221–1230.
3. Ackland DC, Roshan-Zamir S, Richardson M, Pandy MG. Muscle and joint-contact loading at the glenohumeral joint after reverse total shoulder arthroplasty. *J Orthop Res.* 2011;29:1850–1858.
4. Archard JF. Contact and rubbing of flat surfaces. *J Appl Phys.* 1953;24:981–988.
5. Bergmann G, Graichen F, Bender A, Rohlmann A, Halder A, Beier A, Westerhoff P. In vivo gleno-humeral joint loads during forward flexion and abduction. *J Biomech.* 2011;44:1543–1552.
6. Boileau P, Moineau G, Roussanne Y, O'Shea K. Bony increased-offset reversed shoulder arthroplasty: minimizing scapular impingement while maximizing glenoid fixation. *Clin Orthop Relat Res.* 2011;469:2558–2567.
7. Boileau P, Watkinson DJ, Hatzidakis AM, Balg F. Grammont reverse prosthesis: design, rationale, and biomechanics. *J Shoulder Elbow Surg.* 2005;14(1 suppl S):147S–161S.
8. Crosby LA, Hamilton A, Twiss T. Scapula fractures after reverse total shoulder arthroplasty: classification and treatment. *Clin Orthop Relat Res.* 2011;469:2544–2549.
9. DePuy Synthes. Delta Extend™ Reverse Shoulder System. Surgical Technique. Available at: http://synthes.vo.llnwd.net/o16/LLNWMB8/US%20Mobile/Synthes%20North%20America/Product%20Support%20Materials/Technique%20Guides/0612-53-505%20Rev%208_Delta%20XTEND%20Surgical%20Technique.pdf. Accessed August 13, 2015.
10. DJO Surgical. Surgical technique: Reverse® Shoulder Prosthesis. Available at: http://faculty.washington.edu/alexbert/Shoulder/Surgery/EncoreRSPsurgTech.pdf. Accessed August 13, 2015.
11. Ek ET, Neukom L, Catanzaro S, Gerber C. Reverse total shoulder arthroplasty for massive irreparable rotator cuff tears in patients younger than 65 years old: results after five to fifteen years. *J Shoulder Elbow Surg.* 2013;22:1199–208.
12. Giles JW, Degen RM, Johnson JA, Athwal GS. The Bristow and Latarjet procedures: why these techniques should not be considered synonymous. *J Bone Joint Surg. Am.* 2014;96:1340–1348.
13. Giles JW, Ferreira LM, Athwal GS, Johnson JA. Development and performance evaluation of a multi-PID muscle loading driven in vitro active-motion shoulder simulator and application to assessing reverse total shoulder arthroplasty. *J Biomech. Eng.* 2014;136:121007.
14. Grammont PM, Baulot E. Delta shoulder prosthesis for rotator cuff rupture. *Orthopedics.* 1993;16:65–68.
15. Guery J, Favard L, Sirveaux F, Oudet D, Mole D, Walch G. Reverse total shoulder arthroplasty: survivorship analysis of eighty replacements followed for five to ten years. *J Bone Joint Surg Am.* 2006;88:1742–1747.
16. Gutiérrez S, Walker M, Willis M, Pupello DR, Frankle MA. Effects of tilt and glenosphere eccentricity on baseplate/bone interface forces in a computational model, validated by a mechanical model, of reverse shoulder arthroplasty. *J Shoulder Elbow Surg.* 2011;20:732–739.
17. Henninger HB, Barg A, Anderson AE, Bachus KN, Burks RT, Tashjian RZ. Effect of lateral offset center of rotation in reverse total shoulder arthroplasty: a biomechanical study. *J Shoulder Elbow Surg.* 2012;21:1128–1135.
18. Henninger HB, Barg A, Anderson AE, Bachus KN, Tashjian RZ, Burks RT. Effect of deltoid tension and humeral version in reverse total shoulder arthroplasty: a biomechanical study. *J Shoulder Elbow Surg.* 2012;21:483–490.
19. Henninger HB, King FK, Tashjian RZ, Burks RT. Biomechanical comparison of reverse total shoulder arthroplasty systems in soft tissue-constrained shoulders. *J Shoulder Elbow Surg.* 2013;23:e108–117.
20. Inman VT, Saunders JB, Abbott LC. Observations of the function of the shoulder joint. 1944. (The Classic). *Clin Orthop Relat Res.* 1996;330:3–12.
21. Kedgley AE, Mackenzie GA, Ferreira LM, Drosdowech DS, King GJ, Faber KJ, Johnson JA The effect of muscle loading on the kinematics of in vitro glenohumeral abduction. *J Biomech.* 2007;40:2953–2960.
22. Kontaxis A, Johnson GR. The biomechanics of reverse anatomy shoulder replacement: a modelling study. *Clin Biomech.* 2009;24:254–260.
23. Kwon YW, Pinto VJ, Yoon J, Frankle MA, Dunning PE, Sheikhzadeh A. Kinematic analysis of dynamic shoulder motion in patients with reverse total shoulder arthroplasty. *J Shoulder Elbow Surg.* 2012;21:1184–1190.
24. Langohr GD, Giles JW, Athwal GS, Johnson JA. The effect of glenosphere diameter in reverse shoulder arthroplasty on muscle force, joint load, and range of motion. *J Shoulder Elbow Surg.* 2015;24:972–979.
25. Masjedi M, Johnson GR. Alteration of scapula lateral rotation for subjects with the reversed anatomy shoulder replacement and its influence on glenohumeral joint contact force. *Proc Inst Mech Eng H.* 2011;225:38–47.
26. Nam D, Kepler CK, Nho SJ, Craig E V, Warren RF, Wright TM. Observations on retrieved humeral polyethylene components from reverse total shoulder arthroplasty. *J Shoulder Elbow Surg.* 2010;19:1003–1012.
27. Ortmaier R, Resch H, Matis N, Blocher M, Auffarth A, Mayer M, Hitzl W, Tauber M. Reverse shoulder arthroplasty in revision of failed shoulder arthroplasty: outcome and follow-up. *Int Orthop.* 2013;37:67–75.
28. Terrier A, Reist A, Merlini F, Farron A. Simulated joint and muscle forces in reversed and anatomic shoulder prostheses. *J Bone Joint Surg. Br.* 2008;90:751–756.
29. Tornier Inc. BIO-RSA Surgical Technique Manual: Bony Increased Offset - Reverse Shoulder Arthroplasty. Available at: http://www.tornier.com/images/upload/documentation/Epaule/Degenerative_Range/UDRT104_EN.pdf. Accessed August 13, 2015.
30. Walch G, Mottier F, Wall B, Boileau P, Molé D, Favard L. Acromial insufficiency in reverse shoulder arthroplasties. *J. Shoulder Elbow Surg.* 2009;18:495–502.
31. Walpole SC, Prieto-Merino D, Edwards P, Cleland J, Stevens G, Roberts I. The weight of nations: an estimation of adult human biomass. *BMC Public Health.* 2012;12:439.
32. Werner CM, Steinmann PA, Gilbart M, Gerber C. Treatment of painful pseudoparesis due to irreparable rotator cuff dysfunction with the Delta III reverse-ball-and-socket total shoulder prosthesis. *J. Bone Joint Surg. Am.* 2005;87:1476–1486.
33. Woltring H. Data processing and error analysis. In: Berne P, Cappozzo A, eds. *Biomechanics of Human Movement, Applications in Rehabilitation, Sport and Ergonomics.* Worthington, OH: Bertec Corporation; 1990:203–237.
34. Wu G, Van Der Helm FC, Veeger HE, Makhsous M, Van Roy P, Anglin C, Nagels J, Karduna AR, McQuade K, Wang X,

Werner FW, Buchholz B; International Society of Biomechanics. ISB recommendation on definitions of joint coordinate systems of various joints for the reporting of human joint motion. Part II: Shoulder, elbow, wrist and hand. *J Biomech.* 2005;38:981–992.

35. Yang CC, Lu CL, Wu CH, Wu JJ, Huang TL, Chen R, Yeh MK. Stress analysis of glenoid component in design of reverse shoulder prosthesis using finite element method. *J Shoulder Elbow Surg.* 2013;22:932–939.